A Poly-flex Microstrip Patch Antenna for 6G Applications: Design and Performance Analysis under Bending Impact

Salem A. Almazok
Electrical and Electronic Engineering Department, Faculty of Engineering, Alasmarya Islamic University, Zliten, Libya
Email: s.almazok@asmarya.edu.ly

Manuscript received January 23, 2026; revised April 23, 2026; accepted May 29, 2026
*Corresponding author

***Abstract*—Flexible antennas are considered a key enabling technology for next-generation wireless systems, particularly for emerging Sixth-Generation (6G) applications that demand compact, conformal, and mechanically deformable structures. The study presents the design and comparative analysis of a microstrip patch antenna operating at 3 THz, implemented on two polymer substrates: Polyimide (PI) and Polytetrafluoroethylene (PTFE). The antenna performance is investigated using Computer Simulation Technology (CST) Microwave Studio under flat and bent configurations to evaluate its electromagnetic stability under mechanical deformation. The evaluation considers key performance parameters, including return loss (S_{11}), Bandwidth (BW), Voltage Standing Wave Ratio (VSWR), realized gain (G_r), radiation efficiency (η_{rad}), radiation characteristics, and surface current distribution. Bending conditions of 5°, 10°, and 15° are applied across the patch width to simulate realistic deformation scenarios for flexible 6G applications. Simulation results demonstrate that both designs maintain stable electromagnetic performance under bending conditions, with negligible variations in resonance behavior. The PI-based antenna exhibits superior impedance matching, wider bandwidth stability, and improved VSWR performance under deformation, whereas the Polytetrafluoroethylene (PTFE)-based design achieves higher realized gain due to its lower dielectric loss. Radiation efficiency remains consistently stable for both substrates, confirming their suitability for flexible THz applications. The findings highlight the suitability of polymer-based substrates for flexible THz antenna applications and provide practical design insights for selecting appropriate materials in future 6G conformal systems.**

***Index Terms*—Sixth-Generation (6G), Terahertz (THz) band, Microstrip antenna, flexible antenna, polymer substrate**

I. Introduction

The growing demand for higher data rates and ultra-high-speed communications is driving the development of Sixth-Generation (6G) wireless systems, which are expected to be available by 2030 [1]. The Terahertz (THz) frequency band (0.1–10 THz) has emerged as a promising candidate for 6G applications, meeting the performance requirements of future communication networks. It can access much higher bandwidths, exceeding 100 GHz, thereby enabling theoretical 6G data rates of 1 Tbps [1, 2]. Accordingly, research interest in THz communication systems has intensified to exploit the available spectrum and short wavelengths to support a wide range of applications, such as high-speed wireless communications, security systems, medical imaging, spectroscopy, and astronomy [1–3]. Although operating at THz frequencies offers significant benefits, it also poses several challenges that must be addressed, including severe propagation losses, limited transmission distance, high blocking probability, and difficulties in integrating planar electronics with THz antennas [3]. One of the most popular antenna types is the microstrip patch antenna because it is low-profile, lightweight, inexpensive to fabricate, and easily integrates with planar circuits. These benefits make microstrip patch antennas an ideal choice for short-range communication systems in the THz band [3].

In any wireless system, an antenna is an essential component responsible for the effective transmission and reception of electromagnetic waves. Owing to the rapid development of flexible electronics, antenna design has evolved into a flexible, conformal design, giving rise to cutting-edge wearable devices, sensing systems, and next-generation communication platforms [4]. Conventionally, microstrip patch antennas are fabricated by etching conductive materials on a stiff dielectric substrate, such as FR-4 or RT-Duroid. These rigid substrate antennas may undergo permanent deformation if subjected to bending or twisting, resulting in a drastic degradation in performance. Consequently, contemporary communication systems, specifically aimed at 6G and wearable applications, in addition to their requirement for compact and flexible antennas, also require antennas that can be positioned on curved and non-planar surfaces without significant degradation in electromagnetic performance [3, 4].

Flexible antennas can be defined as electromagnetic radiating components that can deform and even bend without losing their mechanical integrity or suffering significant degradation in electromagnetic performance [4]. Unlike rigid antennas, flexible antennas can operate reliably on curved surfaces and are best suited for wearable and portable devices, where they must withstand bending, twisting, and flexing while maintaining a stable operation [3, 4]. In addition to mechanical flexibility, flexible antennas offer numerous

doi: 10.18178/ijeetc.15.4.243-255

benefits, including low-cost fabrication, reduced weight, improved energy efficiency, ease of placement on non-planar surfaces, and seamless integration with microwave components [5]. Such benefits have made flexible antenna design an active research area.

The selection of conductive and dielectric materials is a critical factor in flexible antenna design, as material properties directly influence the efficiency, bandwidth, radiation performance, and mechanical reliability under deformation and bending. In recent years, polymers have attracted significant attention as substrate materials for flexible antenna designs due to their advantages over rigid and textile substrates [4]. Polymer substrates used in flexible antennas typically exhibit high flexibility, relatively low dielectric loss, high glass-transition temperatures, and robust mechanical behavior, making such materials suitable for antennas operating in dynamically deformed or harsh environments [4]. Polymer substrates commonly used in flexible antenna designs include Polyimide (PI), Polytetrafluoroethylene (PTFE, also known as Teflon), Polydimethylsiloxane (PDMS), and Polyethylene Terephthalate (PET) [4].

PI and PTFE have been documented as promising substrates for microstrip patch antennas operating in the THz band. Jayanth *et al*. [6] proposed a microstrip patch antenna resonating at 250 GHz using a PI substrate, confirming the feasibility of polymer-based substrate antennas for THz applications. However, the work was confined to a flat configuration and did not consider the impact of mechanical bending at higher frequencies in the THz range. Belhaouari *et al*. [7] presented a 0.3 THz microstrip patch antenna enhanced with Photonic Bandgap (PBG) structures on a PTFE substrate with Single-Wall Carbon Nanotube (SWCNT) conductors. The proposed optimized antenna performance was enhanced using an AI driving model, and the design achieved a return loss of –26.1 dB, bandwidth of 36.8 GHz, gain of 9.4 dBi, and efficiency of 93.7%. However, although the study used PTFE as a flexible polymer substrate, only a planar configuration was considered, and the effects of mechanical bending were not investigated. Anand *et al.* [8] reported a THz microstrip patch antenna operating at 750 GHz using a PI substrate. The antenna achieved an impedance bandwidth greater than 5% and a peak gain of 5.71 dB at resonance, under planar conditions. However, the performance of the proposed antenna was not evaluated under bending conditions. Ahammed *et al*. [9] proposed a terahertz microstrip patch antenna employing PI substrates for the Internet of Things (IoT) and 6G applications. They showed that machine-learning-based optimization is effective for achieving high gain, efficiency, and a wide bandwidth. However, their work was limited to a planar configuration without considering the impact of bending. Siraj *et al*. [10] proposed a high-performance PI-based substrate patch antenna employing metamaterials for 6G and biomedical technologies. Although the presented work indicates the capability of metamaterials to enhance THz patch antenna parameters, the study was limited to a flat configuration without considering bending.

While most existing studies have focused on the design, simulation, and fabrication of microstrip patch antennas for 6G applications, the impact of mechanical bending on antenna performance has received limited attention. A review of the literature reveals that most research studies primarily utilize rigid dielectric substrates and evaluate electromagnetic performance under planar configurations, whereas mechanical reliability issues, such as bending-induced performance variations, remain inadequately explored, particularly in the THz frequency regime.

In addition, although some studies have addressed the bending effects in flexible microstrip patch antennas, most reported investigations are confined to lower frequency bands, including IoT/wearable applications [11], sub-6 GHz [12], Wi-Fi [13], and sub-6 GHz 5G applications [14]. However, the investigations remain unverified in the THz regime.

Regarding the conductive material selection for the radiating patch, ground, and feed, the selected materials should possess high electrical conductivity, which is a crucial factor for achieving satisfactory performance of the flexible antenna. Furthermore, such materials can endure the performance degradation caused by the various conformal geometries of flexible antennas [4].

While existing studies have investigated mechanical deformation at lower frequency bands [11–14] or assessed THz microstrip antennas solely under flat conditions [6–10], a systematic evaluation of curvature effects in the THz regime has received limited attention. This article addresses this gap by investigating both PI and PTFE substrates under deformation states at the target frequency of 3 THz.

In this study, a flexible microstrip patch antenna operating at 3 THz was designed, simulated, and analyzed for upcoming 6G wireless communication applications. A comparative performance evaluation was conducted using polymer substrates, PI, and PTFE. Furthermore, the mechanical flexibility of the proposed antenna was systematically examined by evaluating its electromagnetic behavior under bending angles of 0°, 5°, 10°, and 15°.

The main contributions of this research can be summarized as follows:

- A flexible microstrip patch antenna operating at 3 THz is designed and analyzed using two polymer substrates, PI and PTFE, to evaluate their suitability for emerging 6G conformal applications.
- A systematic investigation of the bending effect is conducted by analyzing antenna performance under multiple deformation states (0°, 5°, 10°, and 15°), providing a structured understanding of curvature effects at THz frequencies.
- A comparative assessment between PI and PTFE substrates is presented, highlighting material-dependent electromagnetic behavior under bending conditions and offering practical insights for substrate selection in flexible THz antenna design.

The remainder of this paper is organized as follows: Section II presents the materials and methods. Section III details the simulation results, analyses, and performance comparisons. Section IV compares the proposed designs with previous works. Section V discusses fabrication and measurement challenges at THz frequencies. Finally, Section VI concludes the paper and outlines future work.

II. Proposed Antenna Design Methodology

This section outlines the design methodology for the proposed antennas, including the substrate materials and their properties, the antenna geometry, the approach used to simulate curvature at various angles, and the simulation settings used to evaluate antenna performance at terahertz frequencies.

A. *Substrate Materials Characteristics*

Two inset-fed microstrip patch antennas operating at 3 THz are modeled and characterized based on PI and PTFE polymer substrates. The permittivity and loss tangent values of PI used in the simulation are 3.5 and 0.0027, respectively [2, 15, 16]. PI offers a favorable combination of moderate dielectric constant (≈3.5), low-loss tangent (0.0027 at 1 THz), and outstanding mechanical flexibility; these features make it a suitable candidate for flexible, conformal THz microstrip patch antenna design, where mechanical endurance and low dispersion are equally significant [17].

For PTFE, the dielectric constant (ε_r) = 2.10 was adopted from an experimental investigation employing THz time-domain spectroscopy (THz-TDS) published by Ref. [18]. PTFE is considered suitable for high-frequency applications due to its extremely low dielectric constant [19]. In addition, it has a loss tangent (tan δ) of 0.0002, as outlined in a review article [2]. This very low loss tangent value reduces energy dissipation and enhances the radiation efficiency [7].

It should be noted that, due to the limited availability of precise dielectric characterization data at exactly 3 THz, the adopted material parameters are based on well-established values reported in the sub-THz and lower THz ranges. These values have been widely adopted in previous THz antenna studies and are considered acceptable approximations for electromagnetic modeling.

The thermal and environmental stabilities of the proposed substrate materials are essential factors for their practical use in flexible 6G applications under realistic operational scenarios. Based on literature surveys presented in recent peer-reviewed studies [7, 19], both PI and PTFE have been documented to demonstrate promising thermal and environmental features.

In terms of thermal stability, Vineetha *et al*. [19] reported that polyimide exhibits superior thermal stability over a wide temperature range from −200 to 400 °C, making it well-suited for high-temperature applications. Belhaouari *et al*. [7] stated that PTFE offers thermal stability, with a high melting temperature above 327 °C.

Regarding environmental stability, the reported studies demonstrate that polyimides exhibit excellent chemical resistance, rendering them appropriate for harsh environments [19], whereas PTFE exhibits remarkable resistance to corrosive substances [7]. Such material characteristics indicate that both PI and PTFE are appropriate for flexible THz antenna applications in practical scenarios, demonstrating both thermal and environmental stability. The dielectric and thermal properties are summarized in Table I.

Table I: Dielectric and Thermal Properties of PI and PTFE at THz Frequency Region

Material	ε_r	tan δ	Thermal stability	References
PI	3.5	0.0027	−200 °C to 400 °C	[2, 15−17, 19]
PTFE	2.10	0.0002	Melting point > 327 °C	[2, 7, 18]

B. *Rectangular Patch Antenna Design Procedure*

The proposed inset-fed rectangular microstrip patch antenna was designed and simulated using Computer Simulation Technology (CST) Microwave Studio 2022. The proposed antenna structure consists of three main parts: a radiating patch, substrate, and ground plane. The initial dimensions of the antenna were calculated using design relationships for microstrip antennas, and these dimensions were optimized using parametric simulations to achieve the best performance at the operating frequency. Owing to the flexible nature of the proposed antenna and its future applications in 6G systems, two polymer substrates were used.

In both proposed designs, copper is used as the ground plane, whereas silver is used for the patch layer and feed line owing to the high conductivity of these two materials.

The substrate thickness h was determined using the following design Eq. (1) [20]:

$$h \leq \frac{0.3c}{2\pi f_r \sqrt{\varepsilon_r}} \quad (1)$$

where f_r is the resonant frequency (3 THz), c is the speed of light = 3 × 10^8 m/s, and ε_r is the dielectric constant of the used substrate material. The patch width W_p is calculated using the following Eq. (2) [20]:

$$W_p = \frac{c}{2f_r}\sqrt{\frac{2}{\varepsilon_r+1}} \quad (2)$$

The effective dielectric constant $\varepsilon_{\text{reff}}$ can be determined using the following Eq. (3) [20]:

$$\varepsilon_{\text{reff}} = \frac{\varepsilon_r+1}{2} + \frac{\varepsilon_r-1}{2\sqrt{1+12\frac{h}{W_p}}} \quad (3)$$

After calculating $\varepsilon_{\text{reff}}$, the effective length of the patch L_e is calculated using the following Eq. (3) [20]:

$$L_e = \frac{c}{2f_r\sqrt{\varepsilon_{\text{reff}}}} \quad (4)$$

Next, the following relationship is used to determine the length extension ΔL [20]:

$$\Delta L = \frac{0.412 \cdot h(\varepsilon_{\text{reff}}+0.3)\left(\frac{W_p}{h}+0.264\right)}{(\varepsilon_{\text{reff}}-0.258)\left(\frac{W_p}{h}+0.8\right)} \quad (5)$$

Then, the patch length L_p is calculated as follows [20]:

$$L_p = L_e - 2\Delta L \tag{6}$$

The substrate and ground plane dimensions L_s, L_g, W_s, and Wg are calculated using the following Eqs. (7–8) [20]:

$$L_s = L_g = L_p + 6h \tag{7}$$

$$W_s = W_g = W_p + 6h \tag{8}$$

The feed line width W_f is calculated to obtain a 50 Ω characteristic impedance using the following Eq. (9) [21]:

$$W_f = h\left(\frac{377}{50\sqrt{\varepsilon_r}} - 2\right) \tag{9}$$

The feed line length L_f is determined using the following Eq. (10) [20]:

$$L_f = 3h \tag{10}$$

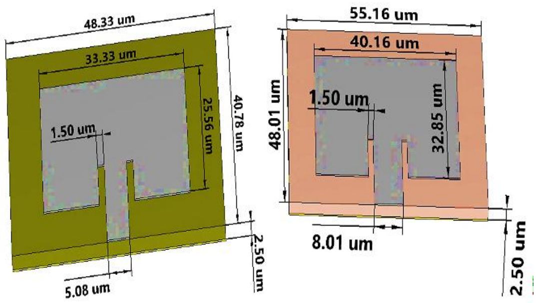

(a) (b)

Fig. 1. Geometry of proposed patch antenna using (a) PI and (b) PTFE substrates.

The simulated structures based on PI and PTFE, resulting from optimized design, are shown in Fig. 1. Table II summarize the dimensions of the proposed structures.

TABLE II: DIMENSIONS OF THE PROPOSED STRUCTURES

Parameter Dimension	PI substrate	PTFE substrate
Substrate Dimension (μm)	48.33 × 40.78 × 2.50	55.16 × 48.01 × 2.50
Patch Dimension (μm)	33.33 × 25.56 × 0.3	40.16 × 32.85 × 0.3
feed line width (μm)	5.08	8.01

C. Equivalent Circuit Model and Bending Impact

The introduced THz inset-feed patch antenna can be theoretically analyzed using a Transmission-Line Model (TLM). Its equivalent circuit model combines the feeding network and radiating slots and is adapted to account for mechanical deformations due to the bending process. This strategy enables a smooth transition from flat configuration to realistic flexible electronics scenarios.

1) Fundamental equivalent circuit

The inset-fed patch antenna, in its initial flat state, is represented by an equivalent circuit that consists of two parallel radiating slots; each slot is represented by a parallel admittance, where the Conductance (G) accounts for radiation and material losses, and the susceptance (B) is associated with fringing fields [22]. Fig. 2 depicts the equivalent circuit of the inset-fed patch antenna using TLM.

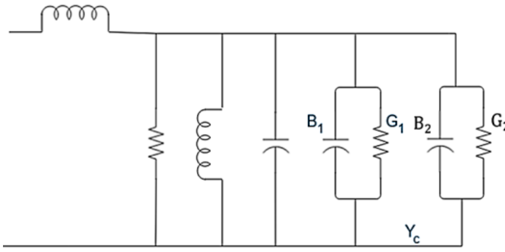

Fig. 2. Equivalent circuit of an insect-fed microstrip patch antenna.

In Fig. 2, Y_C is the characteristic admittance of the feed line, B is the susceptance, and G is the conductance. The conductance G_1 of a single radiating slot can be determined using the following Eq. (11) [22, 23]:

$$G_1 = \frac{1}{120\pi^2}\int_0^{\pi}\left[\frac{\sin\left(\frac{k_0 W_p}{2}\cos\theta\right)}{2\cos\theta}\right]^2 \sin^3\theta\, d\theta \tag{11}$$

where k_0 is the free-space wave number. The feed line impedance (Z_0) and mutual conductance (G_{12}) are determined using the following Eq. (12) [22, 23]:

$$Z_0 = R_{in}\cos^2\left(\frac{\pi y_0}{L_p}\right) \tag{12}$$

where R_{in} is the resonant input impedance, and y_0 is the inset fed position.

$$G_{12} = \frac{1}{120\pi^2}\int_0^{\pi}\left[\frac{\sin\left(\frac{k_0 W_p}{2}\cos\theta\right)}{\cos\theta}\right]^2 J_0(k_0 L_p \sin\theta)\sin^3\theta\, d\theta \tag{13}$$

where J_0 is the zeroth-order Bessel function of the first kind.

In terms of resonant input impedance R_{in}, it is obtained by the following Eq. (14) [22, 23]:

$$R_{in} = \frac{1}{2(G_1 + G_{12})} \tag{14}$$

The inset feed induces a junction capacitance owing to the notch gap, which affects the resonant frequency [23].

2) Equivalent circuit model under mechanical deformation

To integrate flexible antennas into future 6G wireless systems, their mechanical reliability is crucial. The bending mechanism modifies the antenna geometry, primarily affecting the effective patch length and perturbing the electric field distribution between the silver patch and ground plane for both the PI and PTFE substrates [11]. Fig. 3 shows the transformation of the flat patch antenna model into a bent configuration for the bending angles and levels.

To model this behavior accurately, L_p is subdivided into n equal segments, and each segment is interconnected by additional bend-induced capacitance (C_{bend}), which varies with the curvature radius and alters the total susceptance (B), leading to a noticeable shift in the resonant frequency and impedance characteristics. Consequently, the propagation constant (γ) is also modified during bending conditions [11].

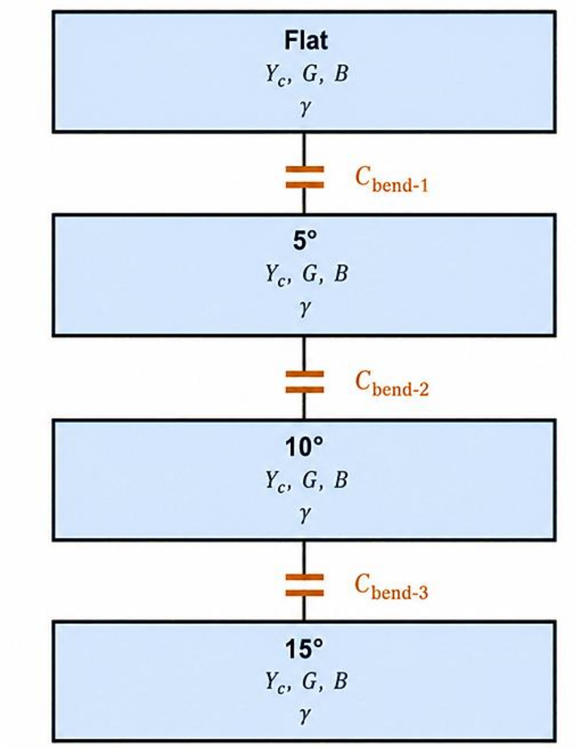

Fig. 3. Equivalent circuit model of the inset-fed microstrip patch antenna under bending conditions.

D. Antenna Bending

Replacing the conventional rigid substrate of an antenna with a flexible substrate has created a new area of research in the field of flexible antenna technology. This is mainly because flexible antennas are designed to be integrated into non-planar and dynamically curved surfaces, which makes bending analysis crucial for evaluating antenna performance. Consequently, the key parameters of the antenna, such as the resonant frequency, reflection coefficient, gain, and radiation efficiency, must be investigated under various bending conditions. This requirement becomes even more significant at THz frequencies, where the extremely short wavelengths make the antenna properties highly sensitive to mechanical deformation. Therefore, in addition to conventional planar antenna analysis, it is crucial to assess the impact of bending on the electromagnetic characteristics of THz flexible antennas to ensure the stable and reliable operation of 6G wireless systems. In this study, bending situations were considered, including 5°, 10°, and 15°. Bending was applied across the patch width to simulate realistic mechanical deformation scenarios for flexible antenna applications. Fig. 4 illustrates the bent configuration of the proposed antennas at a bending angle of 15°, implemented on PI and PTFE substrates.

The following equations were employed to calculate the radius of curvature R resulting from the bending angle θ [14]:

$$S = \theta R \tag{15}$$

$$\theta(\text{Radian}) = \theta(\text{degree}) \times \frac{\pi}{180} \tag{16}$$

$$R = \frac{S}{\theta(\text{Radian})} \tag{17}$$

where S refers to the arc length across the patch width W_p of the proposed antenna.

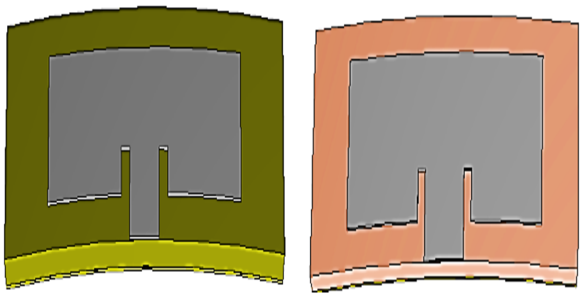

(a) (b)

Fig. 4. Bending configuration of the proposed antennas at 15°: (a) PI, (b) PTFE substrates.

Table III and Table IV summarize the conversion of bending angle (in degrees) into the radius of curvature of the PI and PTFE substrates, respectively.

TABLE III: BENDING ANGLE CONVERSION INTO THE BENDING RADIUS OF PI-BASED SUBSTRATE DESIGN

Bending Angle (θ°)	Angle (θ rad)	Bending Radius (R µm)
5°	0.0872	554.24
10°	0.1745	276.96
15°	0.2617	184.68

TABLE IV: BENDING ANGLE CONVERSION INTO THE BENDING RADIUS OF PTFE-BASED SUBSTRATE DESIGN

Bending Angle (θ°)	Angle (θ rad)	Bending Radius (R µm)
5°	0.0872	632.57
10°	0.1745	316.10
15°	0.2617	210.78

III. SIMULATION RESULTS ANALYSIS AND DISCUSSION

In this section, the two proposed antenna designs were simulated using CST Studio for eight different conditions. The performance parameters, including the return loss (S_{11}), Bandwidth (BW), voltage standing wave ratio (VSWR), realized gain (G_r), radiation efficiency (η_{rad}), radiation pattern, and surface current distribution, were evaluated for the two proposed antennas under flat shape at 0° and bent conditions of 5°, 10°, and 15°.

A. Return Loss and Bandwidth

$S_{11,}$ also known as the reflection coefficient, refers to the amount of power reflected from the antenna [12]. A −10 dB value is considered the reference value for S_{11}, which implies that 10% of the input power is reflected, and 90% is received by the antenna, representing an optimal value for mobile communication [20]. This parameter can be calculated using the following Eq. (18) [12]:

$$S_{11}(\text{dB}) = -20\log_{10}|\Gamma| = -20\log_{10}\frac{v_{ref}}{v_{inc}} \tag{18}$$

where Γ is the reflection coefficient, V_{ref} is the reflected voltage, and V_{inc} is the incident voltage.

B. *Voltage Standing Wave Ratio (VSWR)*

This dimensionless performance parameter for a patch antenna should be less than 2, and its ideal value is 1 [20, 22], indicating how effectively power is delivered to the load from the power source along the transmission line [20]. It is calculated as the ratio between the maximum and minimum standing waves, as presented in Eq. (19) [23]:

$$VSWR = \frac{v_{max}}{v_{min}} = \frac{1+|\Gamma|}{1+|\Gamma|} \tag{19}$$

C. *Realized Gain (Gr)*

The antenna gains G, which is often expressed in dBi and dBd, can be defined as the ratio of the antenna's power density in a desired direction to the power density of the reference antenna at the same point when both antennas are fed with the same power, as shown in the following Eq. (20) [24, 25]:

$$G = \frac{PD.act.ant}{PD.ref.ant} \tag{20}$$

where *PD.act.ant* is the power density of the actual antenna, and *PD.ref.ant* is the power density of the reference antenna with the same input power. In terms of realized antenna gain G_r, it includes the impedance mismatch loss and the antenna efficiency (ohmic losses, etc.), and it is expressed as follows [25]:

$$G_r = G(1 - |\Gamma|^2) \tag{21}$$

D. *Radiation Efficiency (η_{rad})*

This parameter indicates how effectively the antenna radiates and receives electromagnetic waves; therefore, it should be higher for better performance [24]. It represents the ratio of the total radiated power P_r of the antenna to the input power P_{in} fed into the antenna [24]. It can be calculated as follows:

$$\eta_{rad} = P_r/P_{\text{in}} \tag{22}$$

E. *Radiation Pattern and Surface Current Distribution*

The radiation pattern illustrates how the antenna radiates electromagnetic energy with respect to the direction [20]. This indicates the amount of energy radiated by the antenna [24]. It is a key parameter for evaluating antenna performance under mechanical deformation, particularly for emerging flexible 6G applications.

In terms of the surface current distribution of a patch antenna, the current density is expected to be maximal along the radiating edges and minimal at the center of the patch, where the voltage is phase-shifted relative to the current [20].

F. *PI-Based Substrate Antenna Simulation Results*

In Fig. 5, the simulated S_{11} of the proposed PI-based substrate patch antenna under different bending angles is plotted: 0° (flat shape, black line), 5° (blue line), 10° (red line), and 15° (green line). It is observed that all bending conditions resonate around 3 THz, with values that are significantly less than −10 dB. The resonant frequency showed insignificant changes, indicating that the impedance matching under bending remained stable. Furthermore, a slight variation in the return-loss magnitude was observed, with a slight improvement at higher bending angles. This indicates the mechanical robustness and electromagnetic stability of the polyimide substrate, making it a suitable candidate for flexible and wearable 6G devices. In terms of bandwidth, the resulting bandwidth spans approximately from 2.94 THz to 3.05 THz, resulting in a bandwidth of approximately 110 GHz, which offers sufficient spectral capacity to support future 6G applications.

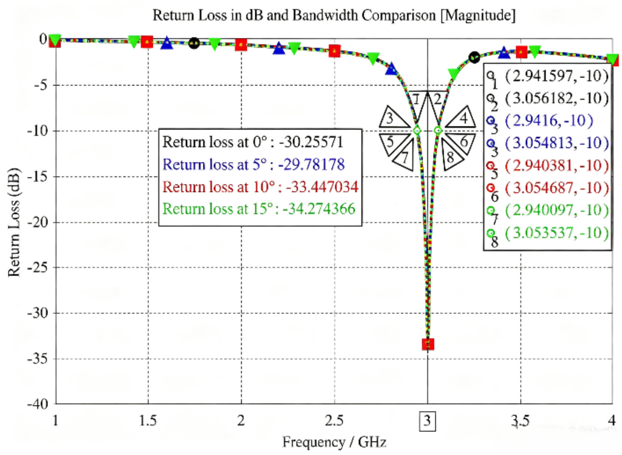

Fig. 5. Bending effect on S_{11} and BW of PI-based substrate antenna.

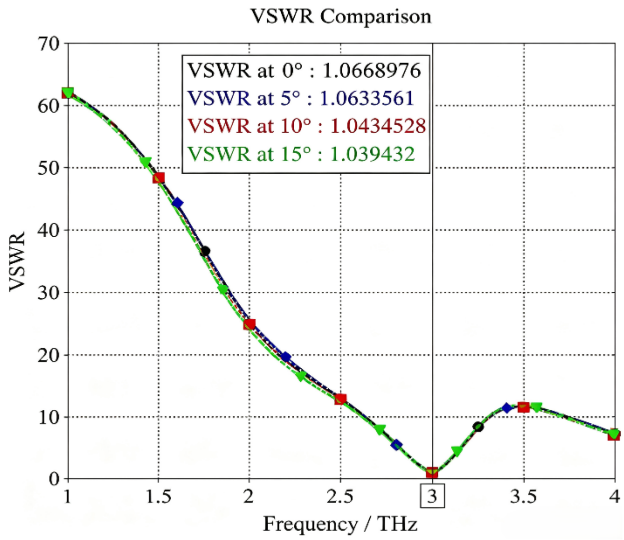

Fig. 6. Bending effect on VSWR of PI-based substrate antenna.

Fig. 6 illustrates the VSWR of the proposed flexible PI-based substrate patch antenna at 3 THz under incremental bending conditions (0°, 5°, 10°, and 15°). The plot shows that the proposed antenna maintains a VSWR close to unity under mechanical bending. The results confirm high mechanical strength and stable operation, which are essential when integrating the antenna with conformal and wearable 6G communication devices that operate on a non-planar surface.

Fig. 7 shows the G_r of the proposed antenna under different bending conditions at 3 THz. It exhibited stable G_r values ranging from 4.4226 to 4.4456 dBi for bending angles of 0°, 5°, 10°, and 15 °, with a maximum variation of 0.023 dBi. This slight variation indicates the stability of the proposed design under mechanical bending, confirming the suitability of the antenna for flexible and conformal 6G applications.

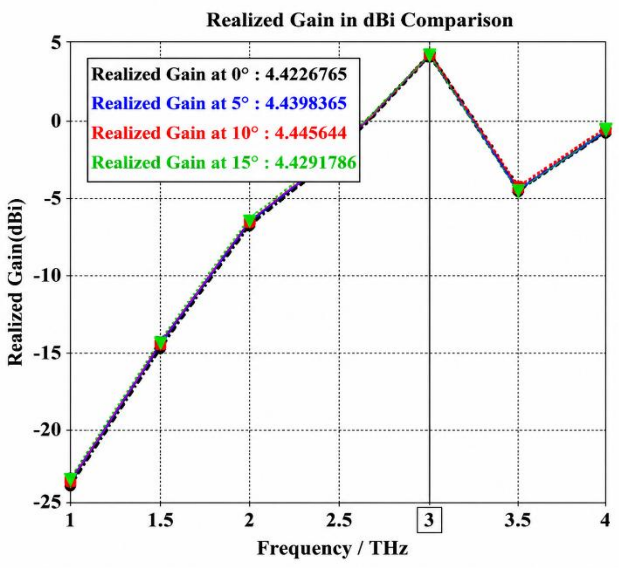

Fig. 7. Bending effect on G_r of PI-based substrate antenna.

Fig. 8 shows the variation in the radiation efficiency of the proposed flexible antenna across the operating frequency range for bending angles of 0°, 5°, 10°, and 15°. The radiation efficiency varied only within a limited range of 61.5% to 62.1% under bending conditions. In particular, this stable performance can be attributed to the relatively low dielectric loss and mechanical flexibility of the employed PI substrate, which help maintain consistent electromagnetic behavior under mechanical deformation.

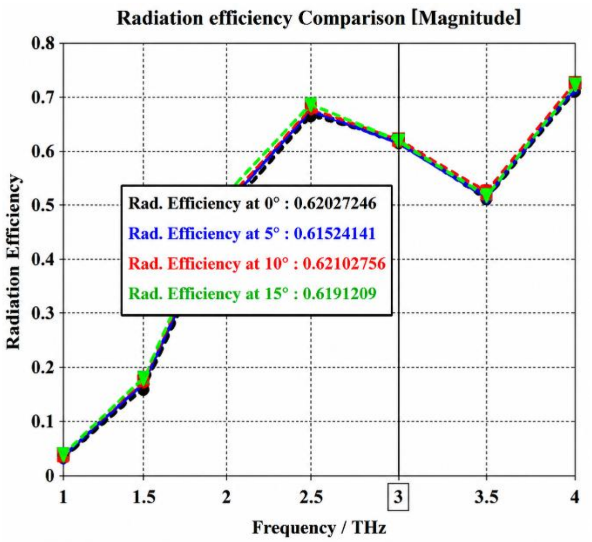

Fig. 8. Bending effect on Rad. Effc. of PI-based substrate antenna.

Fig. 9 shows the radiation patterns of the proposed antenna under flat conditions and at 5°, 10°, and 15° bends in the polar coordinate system. The patterns indicate that the antenna maintains a stable broadside radiation characteristic, as shown by the main lobe direction at 0° across all bending conditions, thus confirming its robustness under mechanical deformation. Furthermore, the half-power beamwidth (HPBW) at the –3 dB level was 93.6° for the flat condition and 91.9°, 93.0°, and 92.7° for the 5°, 10°, and 15° bending conditions, respectively. In addition, the main lobe magnitude values show insignificant variations, ranging from 4.33 dBi to 4.36 dBi for the various bending angles. These results demonstrate that the proposed flexible PI-based substrate patch antenna exhibits robust radiation characteristics under mechanical deformation, making it suitable for integration into upcoming 6G flexible systems.

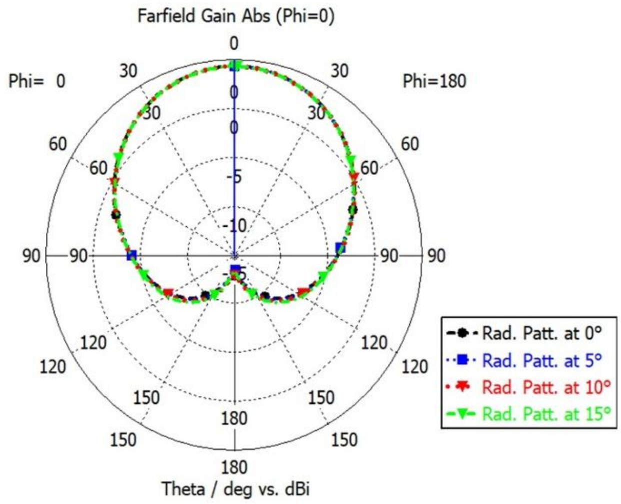

Fig. 9. Bending effect on Rad. Patt. of PI-based substrate antenna.

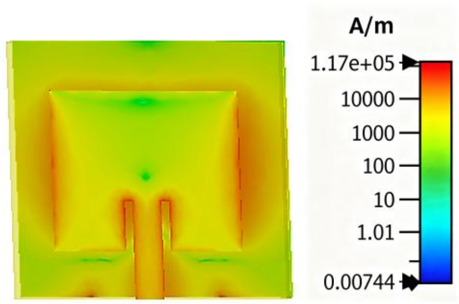

(a)

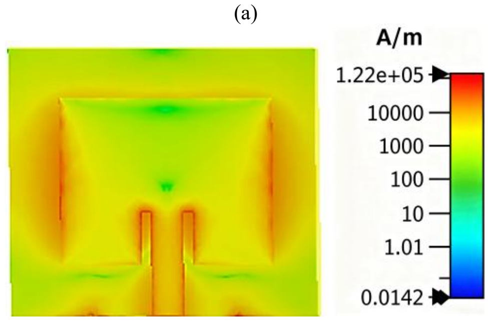

(b)

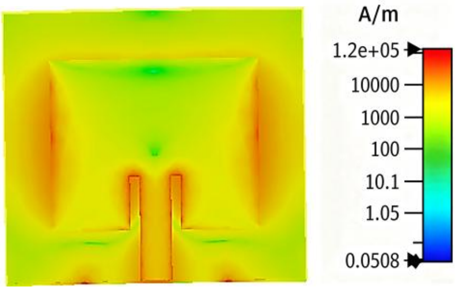

(c)

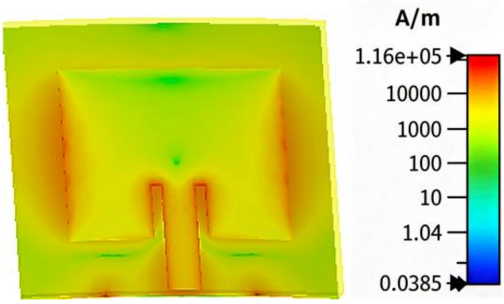

(d)

Fig. 10. Surface current distribution of the proposed PI-based antenna at 3 THz: (a) flat (b) 5° bending angle, (c) 10° bending angle, (d) 15° bending angle.

The surface current distribution of the proposed PI-based antenna was analyzed at a resonant frequency of 3 THz to observe the effect of bending on the current flow. The current distribution was examined at flat and bending angles (5°, 10°, and 15°), as shown in Fig. 10. The results show that the feed line and patch radiating edges are the most critical components for effective radiation, as indicated by their dominant current intensities. Under flat conditions, as shown in Fig. 10(a), the current is concentrated along the feed line and radiating element edges, with the highest intensity indicated at the inset feed region, reaching 1.17 × 10^5 A/m. The current density gradually decreased as the distance from the center of the patch increased. Under bending conditions (Fig.10(b)–(d)), the surface current distribution showed a slight redistribution owing to mechanical deformation. However, the overall pattern remained concentrated along the primary radiating edges, with the maximum current density ranging from 1.16 × 10^5 A/m to 1.22 × 10^5 A/m across all bending angles. This stability confirms the structural robustness of the proposed antenna design for flexible 6G applications.

G. PTFE-based Substrate Antenna Simulation Results

Fig. 11 shows the simulated S_{11} and −10 dB bandwidth of the proposed antenna at various bending angles (0°, 5°, 10°, and 15°). The results indicate that the antenna maintains good matching at the desired resonance of approximately 3 THz under all bending conditions. The lowest loss occurred at a bending angle of 15°, with a value of −27.94 dB. The remaining cases range from −24.37 to −26.52 dB, indicating a highly stable performance. In addition, the resonant frequency changed insignificantly with increasing bending angle, showing a negligible shift around 3 THz. The bandwidth ranges from approximately 3.04–2.94 THz (≈100 GHz) under most conditions, with a slight reduction observed at 10°, where it spans 3.043–2.95 THz (≈90GHz). In general, the results demonstrate that the proposed design has high electromechanical robustness and is suitable for flexible and conformal terahertz applications in next-generation 6G systems, where the design requirements are consistent impedance matching and bandwidth in the presence of mechanical deformation.

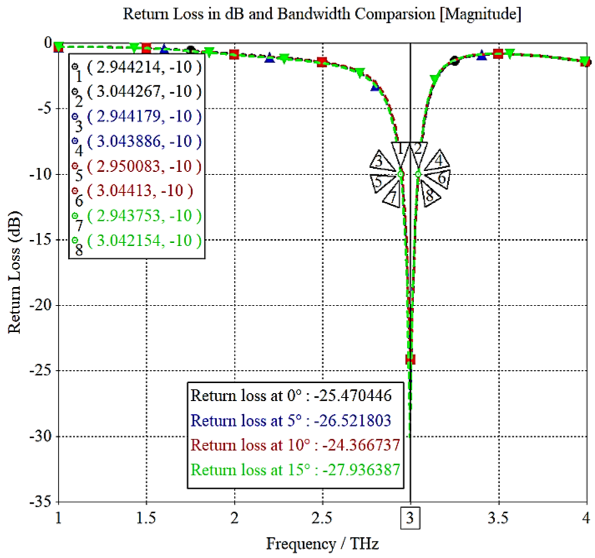

Fig. 11. Bending effect on S_{11} and BW of PTFE-based substrate antenna.

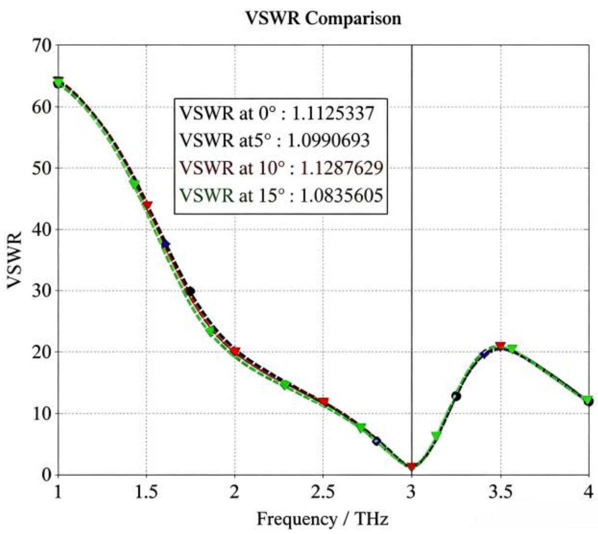

Fig. 12. Bending effect on VSWR of PTFE-based substrate antenna.

Fig. 12 shows the VSWR of the proposed PTFE-based substrate patch antenna at 3 THz under bending angles (0°, 5°, 10°, and 15°). The plot indicates that the proposed antenna provides a VSWR close to the ideal value when mechanically bent. The results demonstrate the suitability of the proposed design when employed with conformal and wearable 6G communication devices that operate on non-planar surfaces.

Fig. 13 shows the *Gr* of the proposed PTFE-based substrate antenna under different bending angles (0°, 5°, 10°, and 15°). The proposed antenna exhibited a consistently good realized gain value of 5.45 dBi at a 0° bending angle, with slight changes across other bending angles. Such stability is essential for flexible and conformal 6G applications.

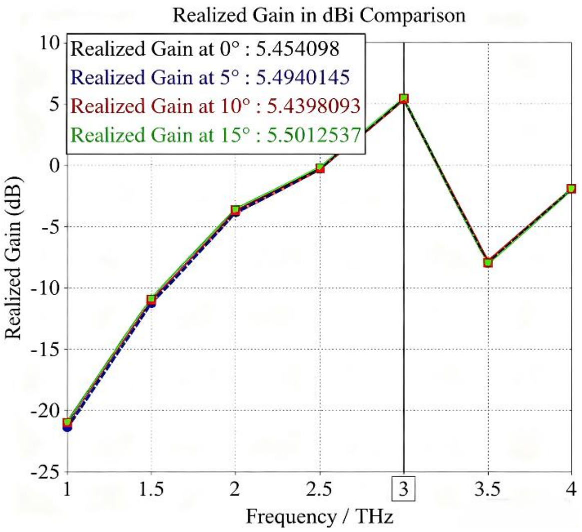

Fig. 13. Bending effect on G_r of PTFE-based substrate antenna.

Fig. 14 shows the radiation efficiency of the proposed flexible PTFE-based substrate antenna for bending angles of 0°, 5°, 10°, and 15°. The bending cases show that the radiation efficiency varies only within a limited range of 61.5% to 63.4% at the resonant 3 THz frequency. This behavior can be attributed to the extremely low loss tangent of the employed PTFE substrate, which limits dielectric dissipation and contributes to preserving efficient electromagnetic performance even under mechanical deformation.

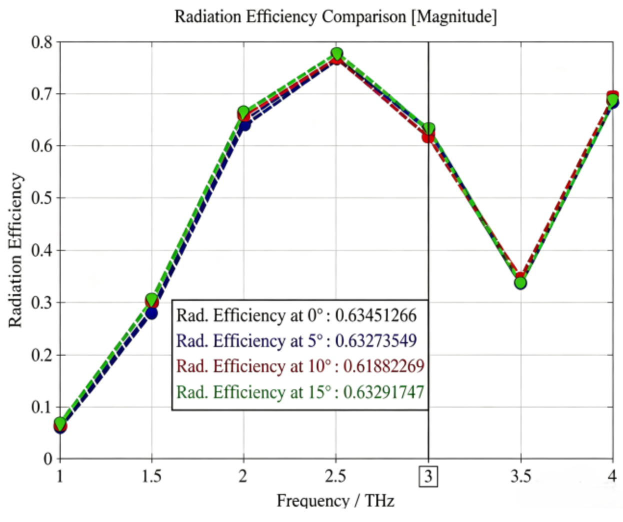

Fig. 14. Bending effect on Rad. Effc. of PTFE-based substrate antenna.

In the polar coordinate system, Fig. 15 shows the radiation characteristics of the proposed antenna in a flat configuration with 5°, 10°, and 15° bends. Among the patterns, the PTFE-based antenna demonstrated stable radiation characteristics, with the main lobe consistently directed at 0° under bending conditions. The angular width (−3 dB level) for the flat shape was 82.5°, whereas for the 5°, 10°, and 15° bends, the widths were 81.5°, 81.1°, and 81.3°, respectively, showing minimal variation under mechanical deformation. The main lobe magnitude remains stable, ranging between 5.23 dBi and 5.36 dBi across all configurations.

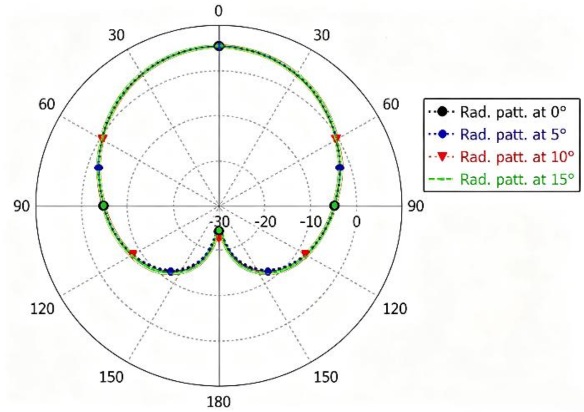

Fig. 15. Bending effect on Rad. Patt. of the PTFE-based substrate antenna.

The surface current distribution of the suggested PTFE-based substrate patch antenna was analyzed at a resonant frequency of 3 THz under flat and bending conditions (5°, 10°, and 15°), as shown in Fig. 16.

Under flat conditions, as illustrated in Fig. 16(a), the current density is concentrated along the feed line and the edges of the patch radiating elements, with the highest current density observed in the inset feed region, reaching 9.9705 A/m. The current density decreases gradually toward the center of the patch, where the minimum current density is 0.00177 A/m.

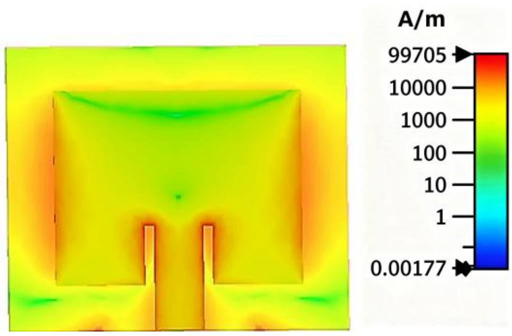

(a)

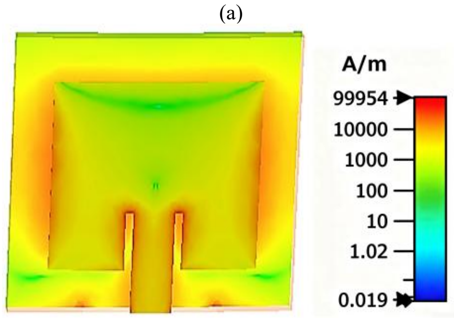

(b)

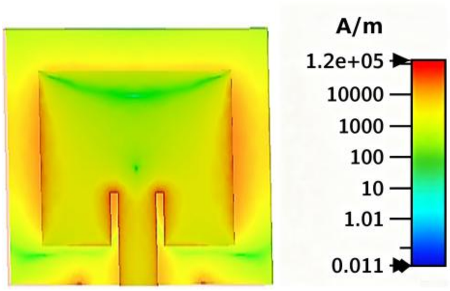

(c)

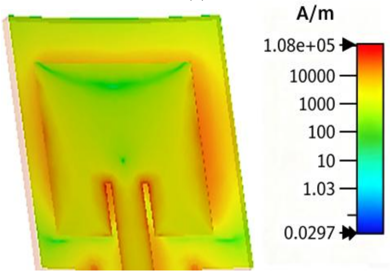

(d)

Fig. 16. Surface current distribution of the proposed PTFE-based antenna at 3 THz: (a) flat (b) 5° bending angle, (c) 10° bending angle, (d) 15° bending angle.

The surface current distribution under bending, as indicated in (Fig. 16(b) to Fig. 16(d)), exhibits slight redistribution due to mechanical deformation. The maximum current density changes between 99954 A/m and 120 × 10^5 A/m throughout bending angles, while the minimum current density ranges from 0.011 A/m to 0.0297 A/m. particularly, at 10° bending angle, the maximum current density reaches its highest value 1.2 × 10^5 A/m, indicating a slight increase in current concentration at the feed point.

Despite slight variation, the overall pattern remained concentrated along the primary radiating edges under all bending states. This consistency confirms that the PTFE-based antenna retains its structural and electromagnetic resilience during deformation, making it suitable for flexible 6G systems.

H. Impact of Bending on Antenna's Resonance Frequency

To quantitatively evaluate the effect of bending on the two-antenna behavior, the resonance frequency at the lowest S_{11} was extracted from the CST simulation data at bending angles of 0°, 5°, 10°, and 15°. Two substrate materials were considered: PI and PTFE.

For the PI-based design, the flat configuration exhibited a resonance frequency of precisely 3 THz. Under bending conditions, the resonance frequency remained at 3 THz at 5° and at 2.998 THz at 10° and 15°. The maximum shift was 0.067%, which is smaller than that of PTFE.

For the PTFE-based antenna, the simulated resonance frequency at 0° was 2.998 THz, deviating approximately by 0.07% from the target design frequency of 3 THz. At bending angles, the resonance frequency exhibited only slight shifts. At 5°, the frequency remained at 2.998 THz. At 10°, the resonant frequency shifted to 3.000 THz, and at 15°, it became 2.995 THz. The maximum shift observed was 0.10% at a bending angle of 15°.

These results demonstrate that both proposed designs maintain a stable frequency behavior under bending angles of up to 15°. These minor shifts fall within the typical numerical accuracy of the CST solver and the mesh resolution. A summary of the resonance frequencies and calculated frequency shifts is presented in Table V and Table VI.

TABLE V: RESONANCE FREQUENCY AND FREQUENCY SHIFT FOR THE PI-BASED ANTENNA

Bending Angle	Resonance Frequency (THz)	S_{11} (dB)	Frequency Shift (%)
0° (Flat)	3.000	−30.26	—
5°	3.000	−29.80	0.00
10°	2.998	−33.47	0.067
15°	2.998	−35.36	0.067

TABLE VI: RESONANCE FREQUENCY AND FREQUENCY SHIFT FOR THE PTFE-BASED ANTENNA

Bending Angle	Resonance Frequency (THz)	S_{11} (dB)	Frequency Shift (%)
0° (Flat)	2.998	−25.96	—
5°	2.998	−27.22	0.00
10°	3.000	−24.37	0.067
15°	2.995	−30.07	0.10

I. Comparative Performance Analysis of Proposed Antenna Designs Under Mechanical Bending

Table VII, Table VIII, and Table IX provide simulated performance metric comparisons for the proposed PI- and PTFE-based substrate patch antennas under flat and bent configurations. Table VII presents the essential performance metrics, including S_{11}, BW, VSWR, G_r, and η_{rad}. Table VIII describes the radiation pattern characteristics, which are the main lobe magnitude, Half-Power Beamwidth (HPBW), and main lobe direction. The surface current distribution characteristics, including the maximum and minimum current densities, and current concentration, are presented in Table IX.

TABLE VII: SIMULATED PERFORMANCE METRICS OF THE PROPOSED PI AND PTFE-BASED SUBSTRATES ANTENNS UNDER BENDING ANGLES

Angle	Substrate	S_{11} (dB)	BW (GHz)	VSWR	G_r (dBi)	η_{rad} (%)
0°	PI	−30.26	116	1.07	4.42	62
	PTFE	−25.47	100	1.11	5.45	63
5°	PI	−29.80	110	1.06	4.44	62
	PTFE	−26.52	100	1.10	5.50	63
10°	PI	−33.45	110	1.04	4.45	62
	PTFE	−24.37	90	1.13	5.44	61
15°	PI	−34.27	110	1.04	4.43	62
	PTFE	−27.94	100	1.08	5.50	63

TABLE VIII: COMPARATIVE ANALYSIS OF RADIATION PATTERN CHARACTERISTICS UNDER FLAT AND BENDING CONDITIONS AT 3 THZ

Angle	Substrate	Main Lobe Magnitude (dBi)	HPBW (deg)	Main Lobe Direction (deg)
0°	PI	4.34	93.6	0
	PTFE	5.33	82.5	0
5°	PI	4.36	91.9	0
	PTFE	5.36	81.5	0
10°	PI	4.36	93.0	0
	PTFE	5.23	81.1	0
15°	PI	4.33	92.7	0
	PTFE	5.35	81.3	0

Throughout the bending scenarios presented in Table VII, the PI-based patch antenna exhibited better impedance matching, with reflection coefficients always below −29 dB and VSWR values close to the ideal value (1.04 to 1.07). Moreover, the PI-based substrate antenna provides a consistent bandwidth between 110 and 116 GHz and an almost constant realized gain of approximately 4.4 dBi. The radiation efficiency is constant at approximately 62% across all bending angles, confirming the robustness and suitability of PI for flexible antenna applications. In comparison, the PTFE-based antenna exhibited a higher realized gain (up to 5.50 dBi) under all bending conditions. However, it has lower impedance matching S_{11} values ranging from −24.37 to −27.94 dB and relatively higher VSWR values. In addition, the bandwidth shows a slight variation with the bending angle, reaching approximately 90 GHz at 10° and about 100 GHz at other angles. It also maintains a stable radiation efficiency (61% to 63%) across all bending angles, indicating stability in the radiation efficiency under mechanical deformation.

In terms of the radiation pattern, as outlined in Table VIII, the PI-based antenna exhibited a stable broadside pattern, with the main lobe direction always at 0° for both flat and bent configurations. The HPBW extends from 91.9° to 93.6°, and the main lobe magnitude remains nearly unchanged between 4.33 dBi and 4.36 dBi under all bending cases. Compared with the PI-based antenna, the PTFE-based antenna has a higher main lobe (up to 5.36 dBi) and a smaller HPBW (81.1° to 82.5°), indicating better directivity and more concentrated energy in the forward direction. However, the PTFE-based antenna exhibited a slightly wider variation (5.23 dBi to 5.36 dBi) in the main lobe magnitude than the PI-based design. The main lobe direction was stable at 0° under all conditions for both substrates, confirming that the pattern was stable under mechanical deformation.

TABLE IX: COMPARATIVE ANALYSIS OF SURFACE CURRENT DISTRIBUTION CHARACTERISTICS UNDER FLAT AND BENDING CONDITIONS AT 3 THZ

Angle	Substrate	Max. Current Density (A/m)	Min. Current Density (A/m)	Current Concentration
0°	PI	1.17×10^5	0.00714	feed line radiating edges
	PTFE	9,9705	0.00177	feed line radiating edges
5°	PI	1.22×10^5	0.0142	feed line radiating edges
	PTFE	9,9954	0.019	feed line radiating edges
10°	PI	1.2×10^5	0.0508	feed line radiating edges
	PTFE	1.2×10^5	0.011	feed line radiating edges
15°	PI	1.16×10^5	0.0385	feed line radiating edges
	PTFE	1.08×10^5	0.0297	feed line radiating edges

Table IX presents the analysis of surface current distribution for both proposed designs, showing that both structures exhibit similar current concentrations along the feed line and the edges of the radiating elements. For the PI-based substrate patch structure, the maximum current density ranges from 1.16×10^5 A/m to 1.22×10^5 A/m across all configurations, while the minimum current density varies between 0.00714 A/m and 0.0508 A/m. In comparison, the PTFE-based substrate patch antenna demonstrates a slightly lower maximum current density, ranging from 9.9705×10^4 A/m to 1.20×10^5 A/m, and a minimum current density between 0.00177 A/m and 0.0297 A/m. Notably, the PTFE-based antenna shows a wider dynamic range between maximum and minimum current densities, particularly under flat conditions. Despite slight redistribution, both proposed structures maintain an overall consistent current pattern across all configurations. This consistency highlights the structural and electromagnetic robustness of both designs for flexible 6G applications.

In summary, both proposed PI and PTFE-based substrate patch antennas are a promising choice for flexible and wearable 6G antenna applications, where structural deformation is inevitable. While PTFE achieves a higher realized gain, PI offers superior mechanical and electromagnetic stability under bending, as demonstrated by improved return loss, bandwidth, and voltage standing wave ratio. Additionally, both designs maintain stable radiation patterns and preserve surface current distribution under bending, confirming their reliability for flexible 6G systems.

IV. COMPARISON OF THE PROPOSED ANTENNA DESIGNS WITH OTHER DESIGNS

To contextualize the proposed antenna structures within previously published research, Table X presents a comparative analysis with earlier flexible and THz patch antenna designs. The comparison focuses on four key elements: operating frequency, substrate material, bending analysis capability, and suitability for emerging 6G applications.

As shown in Table X, previous research evaluating mechanical bending on polymer substrates—such as in references [11, 12]—was limited to GHz frequencies (2.45–7.25 GHz and 5.8 GHz, respectively). While these studies benefit IoT and wearable applications, they do not address the THz band, which is critical for next-generation 6G networks operating above 100 GHz to achieve higher data rates and lower latency.

TABLE X: COMPARISON OF THE PROPOSED ANTENNA DESIGNS WITH PREVIOUS DESIGNS

Ref.	Freq.	Substrate	Bending Analysis	Operates at 6G band
[6]	250 GHz	PI	No	Yes
[7]	0.3 THz	PTFE	No	Yes
[8]	750 GHz	PI	No	Yes
[11]	2.45 GHz	PET	Yes	No
	4.25 GHz	PTFE	Yes	No
	7.25 GHz	PVC	Yes	No
[12]	5.8 GHz	PMMA	Yes	No
This work	3 THz	PI	Yes	Yes
This work	3 THz	PTFE	Yes	Yes

Conversely, THz patch antenna designs in Refs. [6–8] used polymer substrate materials and operated at resonant frequencies of 250 GHz, 750 GHz, and 0.3 THz. However, these studies did not examine the effects of mechanical deformation, as all studies were conducted under flat conditions only.

The present research addresses this gap by systematically investigating bending effects at 3 THz on both PI and PTFE substrates. As highlighted in Table X, previous studies on bending behavior did not consider the THz band [11, 12], while THz designs in Refs. [6−8] focused solely on flat conditions. In this research, the proposed antennas are evaluated at bending angles of 5°, 10°, and 15°, integrating THz operation with bending analysis. This systematic approach distinguishes the current work from prior designs.

V. Fabrication and Measurement Challenges at THz Frequencies

This work is based on full-wave electromagnetic simulations performed using CST Microwave Studio. Experimental validation at THz frequencies is challenging due to limitations in fabrication and measurement infrastructure, and therefore remains outside the scope of this work.

Hajiyat *et al.* [1] convention led fabrication methods for microwave and millimeter-wave antennas are not directly applicable at THz frequencies, as the fabrication process requires extremely high accuracy, tight tolerances, and highly smooth surface finishing. Large surface roughness can increase insertion loss, which impacts antenna performance [1]. Present fabrication techniques for THz band antennas are feasible only for frequencies up to 1 THz, and fabrication technology for frequencies beyond 1 THz remains an active research area [1].

Zandboer *et al*. [26] reported that only 38% of sub-THz antenna structures operating above 200 GHz have been experimentally validated, and this percentage drops to 26% when excluding the ‘other’ antenna categories, which are easier to measure. By comparison, for antennas operating below 200 GHz, 75% of the designs have undergone experimental measurement [26]. Even minor misalignments in measurement setups can result in substantial errors at these short wavelengths [26]. Additionally, within the sub-THz band, the impact of surface roughness becomes more pronounced and can noticeably affect antenna performance, although it remains challenging to model accurately [26]. Furthermore, the electromagnetic properties of materials in the sub-THz band are often not precisely characterized and are typically estimated from lower-frequency data, introducing additional uncertainty into the analysis [26].

Despite these challenges, the simulations in this work employed well-established dielectric values for PI and PTFE from the literature, along with realistic simulation settings. Future experimental investigations, supported by advanced THz fabrication and measurement facilities, are expected to further validate and extend the findings presented in this study.

VI. Conclusion and Future Work

This paper presents a comparative performance analysis of flexible 6G patch antennas implemented on PI and PTFE polymer substrates under bending conditions of 0°, 5°, 10°, and 15°. Antenna performance was evaluated in terms of reflection coefficients, bandwidth, voltage standing wave ratio, realized gain, radiation efficiency, radiation characteristics, and surface current distribution at a resonance frequency of 3 THz. In general, the results confirm that both PI and PTFE substrates enable stable antenna operation during mechanical bending, which is crucial for the advancement of flexible and conformal wireless systems. The PI-based antenna demonstrates superior mechanical and electromagnetic stability at the tested bending angles, exhibiting improved return loss, bandwidth, and voltage standing wave ratio. In contrast, the PTFE-based antenna achieves a higher realized gain. This performance can be attributed to the relatively low dielectric loss tangent of PI and the extremely low loss tangent of PTFE, especially at THz frequencies, contributing to efficient electromagnetic behavior even under mechanical deformation. Frequency shifts under bending remain below 0.1% for both designs, with the PI-based antenna showing slightly better stability (0.067%) compared to PTFE (0.10%). Overall, the comparative analysis suggests that PI substrates offer greater reliability for flexible antenna applications, particularly where mechanical deformation is unavoidable, while PTFE remains a strong alternative when higher gain is desired. These findings provide practical design guidelines for selecting suitable polymer substrates in flexible antenna development for future 6G applications. Future research may focus on experimental validation and further investigations could assess the proposed conformal antennas under greater bending angles and in realistic on-body communication scenarios.

Conflict of Interest

The author declares no conflict of interest.

References

[1] Z. R. M. Hajiyat, A. Ismail, A. Sali, and M. N. Hamidon, “Antenna in 6G wireless communication system: Specifications, challenges, and research directions,” *Optik*, vol. 231, 166415, 2021.

[2] R. Pant and L. Malviya, “THz antennas design, developments, challenges, and applications: A review,” *International Journal of Communication Systems*, vol. 36, e5474, 2023.

[3] A. Youssef, I. Halkhams, R. E. Alami, M. O. Jamil, and H. Qjidaa, “Innovative flexible and compact patch antenna for multiband terahertz applications,” *Scientific African*, vol. 24, e02196, 2024.

[4] P. K. Sharma and J. Y. Chung, “Poly-flex-antennas: Application of polymer substrates in flexible antennas,” *Express Polymer Letters,* vol. 18, pp. 371–390, 2024.

[5] M. U. A. Khan, R. Raad, F. Tubbal, P. I. Theoharis, S. Liu, and J. Foroughi, “Bending analysis of polymer-based flexible antennas for wearable, general IoT applications: A review,” *Polymers*, vol. 13, no. 3, 357, 2021.

[6] J. Jayanth, M. Mahadevaswamy, R. Shreehansa, K. S. Gururaj, and H. K. Ravikiran, “Design and analysis of Sixth-Generation (6G) microstrip patch antenna,” *SN Computer Science*, vol. 4, no. 2, 153, 2023.

[7] S. B. Belhaouari, A. Mokaddem, D. Ziani, M. Belkheir, and M. Rouissat, “ML/GA-based performance optimization of PBG-

enhanced THz microstrip patch antennas on PTFE–SWCNT," *Scientific Reports*, vol. 15, no. 1, 44111, 2025.
[8] S. Anand, D. S. Kumar, R. J. Wu, and M. Chavali, "Graphene nanoribbon-based terahertz antenna on polyimide substrate," *Optik*, vol. 125, no. 19, pp. 5546–5549, 2014.
[9] M. S. Ahammed, R. A. Ananta, J.-J. Tiang, M. Nahas, N. S. S. Singh, and M. A. Haque, "A high-gain THz microstrip patch antenna designed for IoT and 6G communications with predicted efficiency using machine learning approaches," *e-Prime- Advances in Electrical Engineering, Electronics and Energy*, vol. 13, 101058, 2025.
[10] Y. Siraj, Y. Khardioui, K. Saidi Alaoui, and J. Foshi, "High-performance terahertz patch antenna with metamaterials for advanced 6G and biomedical technologies," *Scientific African*, vol. 28, e02716, 2025.
[11] M. U. A. Khan, R. Raad, F. Tubbal, and P. Ioannis Theoharis, "The impact of bending on radiation characteristics of polymer-based flexible antennas for general IoT applications," *Applied Sciences,* vol.11, 9044, 2021.
[12] D. Ziani, M. Belkheir, M. Rouissat, and A. Mokaddem, "Design optimization for microstrip antennas based on polymethyl methacrylate (PMMA) substrate and carbon Nanotube (CNT) conductive material in sub-6 GHz band," *Beni-Suef University Journal of Basic and Applied Sciences*, vol. 13, no. 1, 26, 2024.
[13] S. S. Prabhu, C. Tharini, and M. N. M. Aslam, "Design and performance analysis of WiFi microstrip patch antenna under different bending conditions using flexible substrates," *Engineering, Technology and Applied Science Research*, vol. 14, pp. 16790–16796, 2024.
[14] S. K. Noor *et al*., "A novel experimental design approach to generating orbital angular momentum waves using wearable textile antenna for sub-6 GHz 5G," *PLoS One*, vol. 20, e0310113, 2025.
[15] M. A. Haque *et al*., "Graphene based terahertz MIMO antenna with machine learning regression for 6G communications," *Scientific Reports,* vol. 16, 3900, 2026.
[16] S. M. Alhussini, A. J. Aljohani, and K. H. Alharbi, "Polyimide as antenna substrate for THz InP-based resonant tunnelling diode oscillators," in *Proc. 2021 46th Int. Conf. on Infrared, Millimeter and Terahertz Waves*, 2021, pp. 1−2.
[17] A. S. Mourin, Z. Nishter, and A. Aslam, "Graphene–polyimide flexible electronic platform enabling ultra-broadband high-gain THz MIMO systems," *Advances in Materials Science and Engineering*, vol. 1, 2348309, 2026.
[18] M. S. Islam, J. Sultana, C. M. B. Cordeiro, A. L. S. Cruz, A. Dinovitser, B. W. H. Ng, and D. Abbott, "Broadband characterization of glass and polymer materials using THz-TDS," in *Proc. 2019 44th Int. Conf. on Infrared, Millimeter, and Terahertz Waves (IRMMW-THz)*, Paris, France, 2019, pp. 1−2.
[19] K. V. Vineetha, M. Siva Kumar, B. S. S. Rao, O. P. Kumar, S. R. V, and B. T. P. Madhav, "Design and implementation of a graphene–polyimide-based H-slot terahertz antenna for wireless and biomedical applications," *Plos One*, vol. 20, e0336921, 2025.
[20] R. Przesmycki M. Bugaj, and L. Nowosielski, "Broadband microstrip antenna for 5G wireless systems operating at 28 GHz," *Electronics,* vol. 10, no. 1, 1, 2020.
[21] M. K. Azizi, M. A. Ksiksi, H. Ajlani, and A. Gharsallah, "Terahertz graphene-based reconfigurable patch antenna," *Progress in Electromagnetics Research Letters,* vol. 71, pp. 69–76, 2017.
[22] A. Matinm and I. Sayeeda, "A design rule for inset-fed rectangular microstrip patch antenna," *WSEAS Trans. on Communications*, vol. 9, pp. 63–72, 2010.
[23] K. Singh, M. Dhayal, and S. Dwivedi, "Design and analysis of ultra-wideband microstrip patch antenna with various conductive materials for terahertz gap," *Discover Applied Sciences*, vol. 6, no. 224, 2024.
[24] S. A. Almazok, A. O. Mami, and S. A. M. Aldrewy, "Performance comparison of 28 GHz rectangular patch antenna based on three different dielectric constant substrates for 5G communications," *International Journal of Engineering and Information Technology,* vol. 11, pp. 1–6, 2023.
[25] R. B. Keller, *Design for Electromagnetic Compatibility−in a Nutshell*, 2023, pp. 111–134.
[26] J. C. F. Zandboer, G. Federico, U. Johannsen, and A. Bart Smolders, "A review on antenna technology developments for sub-THz wireless communication: application, challenges and opportunities," *IEEE Open Journal of Antennas and Propagation,* vol. 6, pp. 645–663, 2025.

Salem A. Almazok received the B.Sc. degree in electrical and electronic engineering (communication engineering) in 2007 from Bani Walid Higher Institute of Electronics, Libya (currently the Technical College). He obtained the M.Sc. degree in electrical and electronic engineering from Griffith University, Australia, in 2013, and the Ph.D. degree from Near East University, Northern Cyprus, in 2020. He is currently an assistant professor at the Faculty of Engineering, Alasmarya Islamic University, Libya. His research interests include microstrip patch antenna design, terahertz (THz) patch antenna for next 6G wireless communication systems.